Progress In Electromagnetics Research B, Vol. 25, 113–130, 2010

PERFORMANCE EVALUATION OF PHASE-ANGLE GRADIENT METHOD FOR PHASE RETRIEVAL BASED ON LOW-FREQUENCY AMPLITUDE-ONLY NEAR-FIELD DATA

M. Johansson, H.-S. Lui, and M. Persson

Department of Signals and Systems
Chalmers University of Technology
SE 41296, Gothenburg, Sweden

Abstract—The Phase Angle Gradient Method (PAGM) is a recent technique developed for phase retrieval based on amplitude-only measurement data. Preliminary results have shown that the PAGM is able to perform phase retrieval at 100 MHz with accurate phase information based on measured field components on three planar surfaces. In this paper, a performance evaluation of the PAGM under different configurations is conducted. Phase retrieval based on field measurements for different plane sizes and separations between the planes are studied rigorously. In addition, the PAGM is tested for different initial phase distributions. The results show that the PAGM is capable of retrieving phase information even if the separation between the measurement planes is small in terms of wavelengths.

1. INTRODUCTION

In the last two decades, there have been extensive studies in the area of accurate near-field measurements. One of the most well known applications is to compute the far-field radiation pattern of an antenna under test (AUT) using measured near-field data. Although different methods exist to synthesize radiation patterns, see for example [1], it is also of large interest to be able to find the radiation pattern from measured near-field. AUT measurements are often conducted in indoor environments such as anechoic chambers. In general, anechoic chambers are designed with the available building space and

Received 2 July 2010, Accepted 19 August 2010, Scheduled 25 August 2010
Corresponding author: M. Johansson (markusjo@chalmers.se).

measurement-hardware limitations. If near-field is measured instead of far-field, the space required for the measurements can be considerably decreased.

Given the measured near-field data, the far-field information can be obtained via a near-field far-field (NF-FF) transformation. For a standard NF-FF transformation, both amplitude and phase of the near-field data is required. In practice, however, accurate measurements of amplitude and phase generally require more efforts and more expensive hardware than phaseless measurements. As a result, researchers have been looking into methods to retrieve the phase information based on amplitude-only measurements and reconstruct the far-field radiation pattern [2–6]. Phase retrieval methods are not only limited to NF-FF transformations and antenna diagnostics. In general, they are useful for modeling of field distributions from electromagnetic sources. Recent efforts have also been contributed to millimeter-wave imaging applications in which the phase information of the scattered field is retrieved based on amplitude-only measurements [7]. In [8] a phase retrieval method applied to infrared near-field measurements is discussed.

There are a number of different methods in the area of phase retrieval based on amplitude-only measurements. Isernia et al. [2, 3] have proposed a phase-retrieval method which searches for the complex electric field that gives measured field amplitudes on two planes. A cost function that relates the differences between the estimated electric field and the measured amplitudes is defined in such a way that the inverse problem becomes quadratic. The cost function is minimized with a conjugate gradient method. Rahmat-Samii et al. [4, 5] have proposed another method, known as the Bi-Polar phase-retrieval algorithm. In that method the unknown phase information is searched for in a forward-backward propagation manner.

Instead of using the forward and backward propagation manner, Las-Heras and Sarkar [6] has proposed a direct optimization approach. In this method the electromagnetic source is represented by an equivalent magnetic current distribution on a surface in front of the source. The magnetic current distribution can be written as a sum of basis functions with unknown coefficients. So, instead of seeking the unknown electric field components directly, the unknown expansion coefficients are searched for. A cost function that relates the differences between the measured amplitudes and the amplitudes of the estimated field, that the expansion coefficients give, is minimized. The minimization is performed with a conjugate gradient algorithm.

The phase retrieval algorithms described above use field measurements from two planar or circular surfaces and the separation

between the surfaces is normally larger than a wavelength λ. A summary of the examples presented in [2–7] are given in Table 1. It is clearly shown that phase-retrieval are usually performed with plane sizes in the scale of 10λ and separation distances of a few wavelengths between the planes are normally used. For operating frequencies at

Table 1. Summaries of the Phase Retrieval examples presented in [2–7]. d_1 is the distance between the source and plane 1 (line 1), d_2 correspond to the distance between planes (lines) 1 and 2 and d_3 corresponds to the distance between lines 2 and 3. r_1 and r_2 are the radius of the circular ring and l_1, l_2 and l_3 are the lengths of the lines.

	Number of planes	Plane size	Separations between the planes	Frequency
[2]	2	$16\lambda \times 16\lambda$	$d_1 = 5\lambda$ $d_2 = 10\lambda$	Not specified
[3]	2	$54\lambda \times 54\lambda$	$d_1 = 1.26\lambda$ $d_2 = 5.31\lambda$	9 GHz
[4]	2	Not specified	$d_1 = 4.17\lambda$ $d_2 = 2.36\lambda$	9.3 GHz
[5]	2	Measured in circular ring with radius $r_1 = 19.318\lambda$ $r_2 = 22.5\lambda$	$d_2 = 2.581\lambda$	9.375 GHz
[6]	Example 1: 2 Planes	$8\lambda \times 8\lambda$	$d_1 = 2\lambda$ $d_2 = 2\lambda$	Not specified, simulation
[6]	Example 2: 2 Planes	$8\lambda \times 8\lambda$	Not specified	Not specified, simulation
[6]	Example 3: 3 lines (1D problem)	$l_1 = 5\lambda$, $l_2 = 10\lambda$ $l_3 = 20\lambda$	$d_1 = d_2 =$ $d_3 = 20\lambda$	Not specified, simulation
[6]	Example 4: 2 Planes	0.88 m × 0.88 m ($37.03\lambda \times 37.03\lambda$)	$d_1 = 40$ cm (16.83λ) $d_2 = 100$ cm (42.083λ)	Aperture antenna + reflector at 12.625 GHz
[7]	2	$32\lambda \times 32\lambda$	$d_1 = 6.5\lambda$ $d_2 = 3.5\lambda$	Phase retrieval of scattered field in THz region

around 10 GHz ($\lambda \approx 3$ cm), the physical distance of a few wavelengths can easily be achieved in practice. However, if the operation frequency is significantly reduced to MHz or even nearly to DC, phase retrieval in the region of a few wavelengths separation can be much harder to achieve.

In view of this, Johansson et al. [9] have recently proposed another phase retrieval method known as the Phase Angle Gradient Method (PAGM). Preliminary results have demonstrated that the method is able to perform phase retrieval at 100 MHz [10]. In this paper, further work has been conducted and the performance of the PAGM for different sources and configurations is investigated. The objective here is to investigate the limits for what the PAGM can perform. This is very important if one wants to perform phase retrieval when the measurement points are close to the source (closer than one wavelength), especially when the operation frequency is so low that measurements at a distance of a few wavelengths are not easily achievable in practice. To our knowledge, phase retrieval under such configuration has not been widely reported in the open literature. Therefore, the performance of phase retrieval for different planar sizes and separations, as well as different initial phase distributions for the optimization process, is studied in detail.

The paper is outlined as follows. A review of the PAGM will be given in the next section, followed by the numerical examples in Section 3. Discussions of the results will be given in Section 4 and conclusions will be reached towards the end of the paper.

2. THE PHASE ANGLE GRADIENT METHOD

According to the field equivalence principle, an electromagnetic source can be replaced by an equivalent source as illustrated by Figure 1 [11]. The equivalent in the figure consists of a perfect electric conductor (PEC) and a magnetic surface current density $\bar{M}_{eq}$ on the surface of the PEC S_c. If S_c encloses the volume that the actual source would occupy in the real case and

$$\bar{M}_{eq} = -\hat{n} \times \bar{E}_1, \tag{1}$$

where $\hat{n}$ is a unit normal pointing out from S_c and $\bar{E}_1$ is the electric field that the actual source would give on S_c, the resulting field outside S_c would be the same as for the actual source.

The surface S_c can be chosen so that part of it is a very large plane surface parallel to and close to plane 1. The field from the equivalent, in Figure 1, can then be approximated with the field from a magnetic surface current density on plane 1 in front of an infinite PEC plane, if

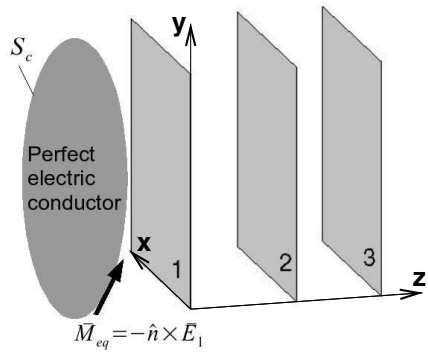

Figure 1. Equivalent, that can replace an electromagnetic source, in front of planes where field amplitudes can be measured. The equivalent gives the same field outside the surface S_c as the actual source.

plane 1 is large enough. By using mirroring it can therefore be realized that the actual electromagnetic source can be replaced by an equivalent magnetic surface current density on plane 1

$$\bar{M}_s = -2\hat{n} \times \bar{E}_{p1}, \tag{2}$$

where $\hat{n}$ is a unit vector perpendicular to plane 1 pointing towards the other planes and $\bar{E}_{p1}$ is the total electric field on plane 1.

One can divide plane 1 into a square grid with the grid cell area ΔS. If the point in the middle of the square number p is represented by $\bar{r}'_p$, the Cartesian components of the electric field $\bar{E}$ in any point $\bar{r}$ on the other measurement planes can be calculated [9] with the expressions

$$E_x(\bar{r}) = -\frac{\Delta S}{2\pi} \sum_p E_x\left(\bar{r}'_p\right) \frac{\partial G\left(\bar{r}, \bar{r}'_p\right)}{\partial z} \tag{3}$$

$$E_y(\bar{r}) = -\frac{\Delta S}{2\pi} \sum_p E_y\left(\bar{r}'_p\right) \frac{\partial G\left(\bar{r}, \bar{r}'_p\right)}{\partial z} \tag{4}$$

$$E_z(\bar{r}) = \frac{\Delta S}{2\pi} \sum_p \left(E_x\left(\bar{r}'_p\right) \frac{\partial G\left(\bar{r}, \bar{r}'_p\right)}{\partial x} + E_y\left(\bar{r}'_p\right) \frac{\partial G\left(\bar{r}, \bar{r}'_p\right)}{\partial y} \right). \tag{5}$$

Here the system of coordinates is chosen, as illustrated in Figure 1, such that plane 1 is on the x-y plane and $G(\bar{r}, \bar{r}')$ is the Green's function

$$G\left(\bar{r}, \bar{r}'\right) = \frac{e^{-jk|\bar{r}-\bar{r}'|}}{|\bar{r}-\bar{r}'|}, \tag{6}$$

where k is the wavenumber. If ΔS is small enough and plane 1 sufficiently large, Equations (3), (4) and (5) give a good approximation for the electric field on the other planes. Since the field amplitudes on plane 1 can be obtained from measurements, $\bar{E}$ on the other measurement planes can be regarded as a function of the unknown phase angles of the tangential field components on plane 1.

The objective of the PAGM is to retrieve the phase information of $\bar{E}$ on plane 1. After the phase angles on plane 1 have been set to an initial phase distribution, the resulting field estimates on the planes 2 and 3 can be calculated. To find the correct phase distribution, the initial phase angles are altered in small steps, so that the field amplitudes $|E_i|_n$ converge to the measured values $|E_i^m|_n$. Here n is a computational grid point on plane 2 or 3. A cost function of the phase can be defined as

$$J \equiv \frac{1}{2} \sum_n \left((|E_x|_n - |E_x^m|_n)^2 + \left(|E_y|_n - |E_y^m|_n\right)^2 + (|E_z|_n - |E_z^m|_n)^2 \right). \quad (7)$$

The phase angles are changed in the opposite direction of the phase angle gradients of the cost function J, so that J is minimized. That is, in each iteration the phase angles for the x- and y-components of the field in each grid cell on plane 1 are updated according to the equation

$$\phi^{new} = \phi^{old} - G_\phi^{old} \cdot \alpha, \quad (8)$$

where ϕ^{old} and ϕ^{new} are the values of a phase angle ϕ before and after the update. G_ϕ^{old} is

$$G_\phi = \frac{\partial J}{\partial \phi} \quad (9)$$

calculated for the values of the phase angles on plane 1 before the update and α is a constant, that is chosen with a line search method.

To quantify results for the phase-retrieval, the summed and weighted phase angle error

$$\phi_{err} = \sqrt{\frac{\sum_n \left(|E_x|_n^2 \left(\phi_{x,n}^{diff}\right)^2 + |E_y|_n^2 \left(\phi_{y,n}^{diff}\right)^2 \right)}{\sum_n \left(|E_x|_n^2 + |E_y|_n^2 \right)}} \quad (10)$$

can be calculated. Here, $\phi_{x,n}^{diff}$ is the error in the calculated phase angle for E_x in the measurement point on plane 2 or 3 with number n and $\phi_{y,n}^{diff}$ is the corresponding error for E_y. The average is weighted with the amplitudes, since it is more important that errors are small in places where the amplitude is large, than in places with small amplitudes. If an unessential constant phase is added to all the

obtained phase angles, the resulting phase is neither better nor worse, but the resulting summed and weighted phase angle error can become different. So to try to get a fair measure of how good the resulting phase is, the constant phase that gives the smallest ϕ_{err} if added to the calculated phase, is numerically searched for. The ϕ_{err} that is obtained for the found constant phase, when it is added to the calculated phase, is the value that then is used.

3. NUMERICAL TEST CASES

The PAGM was previously tested for a few test cases, with an infinitesimal dipole as the source, in [10]. This is a very suitable source to start with, however, to evaluate the PAGM further it is also of large interest to test it with some different source. This is done in Subsection 3.1. Moreover it is interesting to evaluate the performance of the method for test cases with different sizes in terms of wavelengths. In Subsection 3.2 the PAGM is tested for test cases with relevant dimensions ranging from extremely small compared to λ to comparable to λ.

3.1. Source Consisting of Five Dipoles

In order to extend the work in [10], where the PAGM was tested with an infinitesimal dipole source, the method was tested with a source that consists of five infinitesimal dipoles.

Field amplitudes calculated with analytical formulas on three parallel measurement planes in front of the source, see Figure 1, were used to calculate the phase angles. The right-angled distance between the centre of the plane and the middle of the source was 0.1λ. All the five infinitesimal dipoles in the source were parallel to the y-axis. One dipole was placed in the centre of the source. The other four dipoles were placed 0.05λ in negative x-direction, 0.05λ in positive x-direction, 0.05λ in negative y-direction and 0.05λ in positive y-direction, respectively, from the centre dipole, see Figure 2. The currents of the four dipoles were -0.5, 0.5, -0.5 and 0.5 times the current of the centre dipole, respectively.

Field values from 100×100 measurement points on plane 1 and 60×60 measurement points on each of the other two planes were used. The distances between the points on each plane in x as well as y-direction were 0.01λ. From plane 1 to plane 2 and from plane 2 to plane 3 the distances were 0.1λ and 0.05λ, respectively.

The phase angles obtained with the PAGM and the correct phase angles from the analytical formulas, for E_x and E_y on plane 1 are

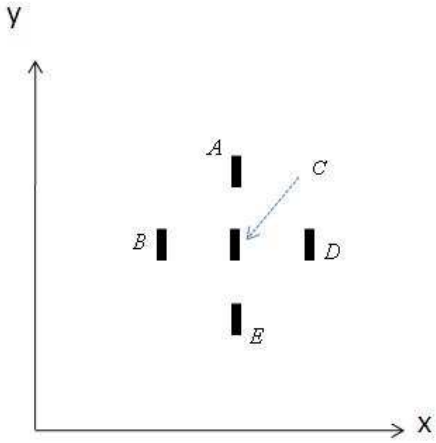

Figure 2. The five-infinitesimal-dipole source used in the first test case. The relative amplitudes with respect to source C for the other sources are $A = 0.5$, $B = -0.5$, $D = 0.5$ and $E = -0.5$. Each dipole source is radiating at 100 MHz.

shown in Figure 3. The differences between retrieved and correct phase is shown in the figure as well. It can be seen in Figures 3(a), (b), (d) and (e) that the PAGM gives phase angles that are similar to the correct ones. Figures 3(c) and (f) illustrate that for both E_x and E_y the differences between calculated and correct phase angles are small, with the exception of some unimportant larger errors in areas near rapid changes in the phase and near the edges of the planes.

Figure 4 shows the correct field amplitudes for E_x and the differences between calculated and correct phase angles for E_x, on plane 1. Small errors in the calculated phase can be observed at places where the field amplitudes are large. Larger errors can be seen at places with smaller amplitudes where the value of the phase not is important. It is also reasonable that the error in such places are larger, since they do not change the minimized functional much. Figures 5 and 6 show retrieved and correct phase for E_x and E_y. It can be seen that the retrieved phase for both E_x and E_y are very close to the correct phase. This shows that the PAGM is able to retrieve the phase on plane 2 and it also shows that the errors in plane 1 do not significantly affect the accuracies of the retrieved phase on plane 2.

The result in the Figures 3 and 4 were obtained for the initial value zero for each of the phase angles on plane 1. To verify that the PAGM works well for different initial phase distributions, the method was also

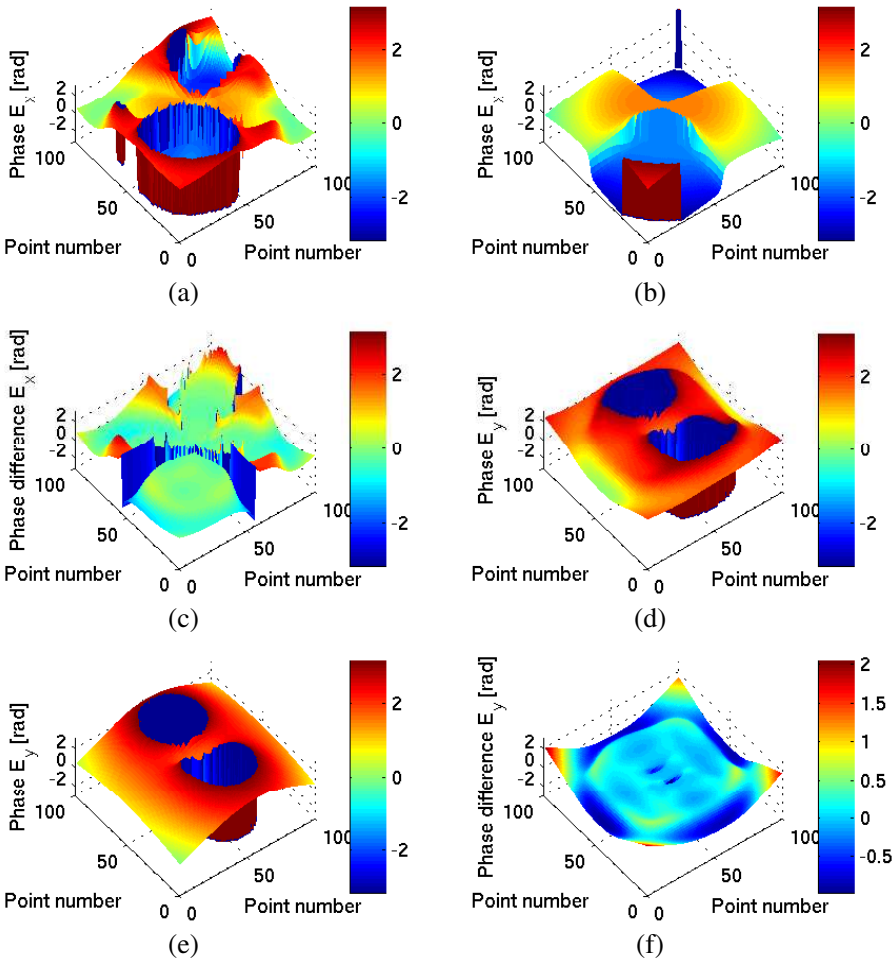

Figure 3. Phase angles obtained with the PAGM for source consisting of five infinitesimal dipoles, correct phase angles and the difference between them. (a) Retrieved phase for E_x. (b) Correct phase for E_x. (c) Phase difference for E_x. (d) Retrieved phase for E_y. (e) Correct phase for E_y. (f) Phase difference for E_y. To facilitate comparison between retrieved and correct phase, all the axes for the phase and the colorbars in (a), (b), (d) and (e) have the same max and min. The colorbars for (c) and (f) have maxima and minima that are chosen to make it possible to see how the differences varies.

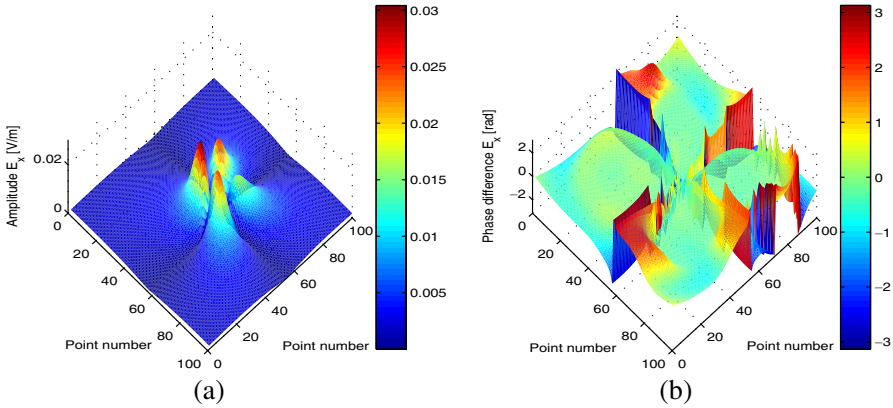

Figure 4. (a) Correct field amplitudes for E_x on plane 1. (b) Differences between calculated and correct phase angles for E_x on plane 1.

tested for an initial phase distribution where the phase in each point was set to a random number. Figure 7 shows the cost function J as function of iteration number for the cases with initial phase zeros and initial phase random numbers. The summed and weighted phase angle errors as defined in Equation (10) as functions of iteration numbers for the two initial phase distributions can also be found in Figure 7. It can be seen that the two curves for the cost function J starts differently, but when the number of iterations becomes large enough they reach similar values. Moreover the resulting summed and weighted phase angle errors are low for both the initial field distributions, so the PAGM works well for both cases.

3.2. Test Cases with Different Plane Sizes and Separations

The PAGM was also tested for some other different test cases, to verify that it can be used in situations with smaller and larger distances in terms of wavelengths. The source for the test cases was an infinitesimal dipole operating at 50 Hz and pointing in the y-direction in the coordinate system in Figure 1. Field amplitudes from analytical formulas on three parallel measurement planes in front of the dipole were used to calculate the phase angles.

For the initial test case, the right-angled distance between the centre of plane 1 and the source was 5 cm ($\approx 8.3 \times 10^{-9}\lambda$). On plane 1 field values from 100×100 measurement points were used and on each of the other two planes 60×60 points were used. The distance between

the points on each plane in x as well as y-direction was 0.5 cm. From plane 1 to plane 2 and from plane 2 to plane 3 the distances were 5 cm and 2.5 cm respectively.

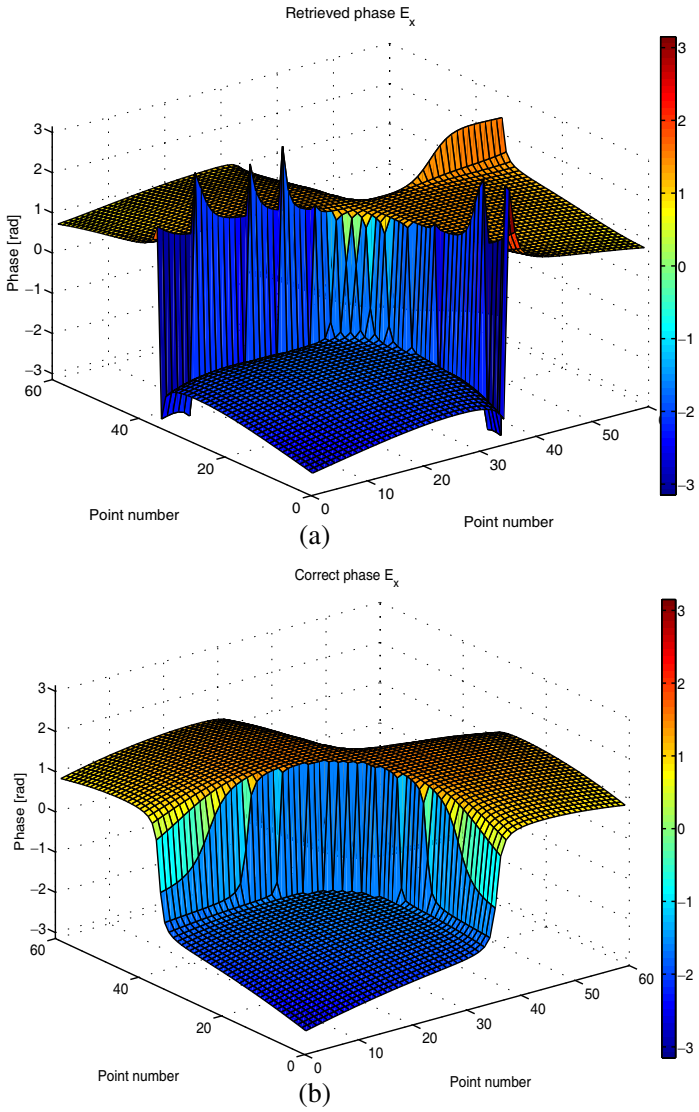

Figure 5. (a) Retrieved phase for E_x plane 2. (b) Correct phase for E_x plane 2.

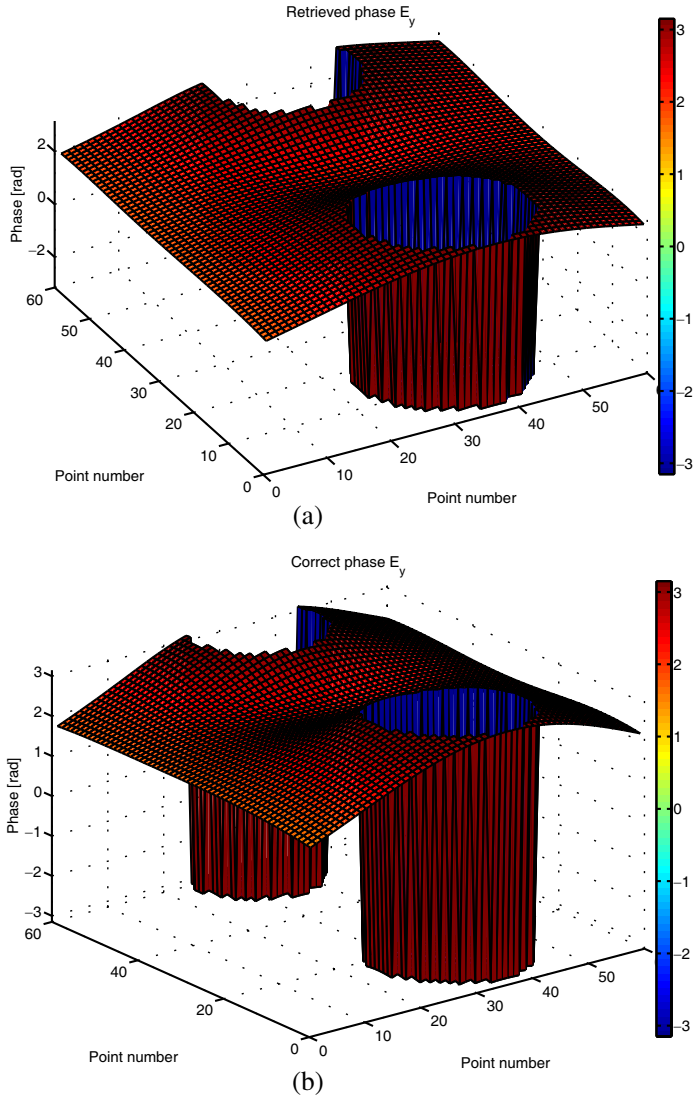

Figure 6. (a) Retrieved phase for E_y plane 2. (b) Correct phase for E_y plane 2.

The dimensions for the initial test case, see Figure 1, except the source, were then increased with the same scale factor. That is the sides of the measurement planes, the distances between them as well as the distance to the source from the planes, were all scaled up by the

same factor, while the same source as in the first test case was kept. In the following test cases, the source is maintained to be the same unless otherwise stated.

Figure 8 shows obtained summed and weighted phase angle error ϕ_{err} for different scaling factors. The results are shown as function of the distance between plane 1 and plane 2. The result for the initial test case is indicated as A in Figure 8. The figure shows small errors for distances between plane 1 and plane 2 that are smaller than 0.5λ. For the distances 0.5λ and 0.7λ the errors are larger.

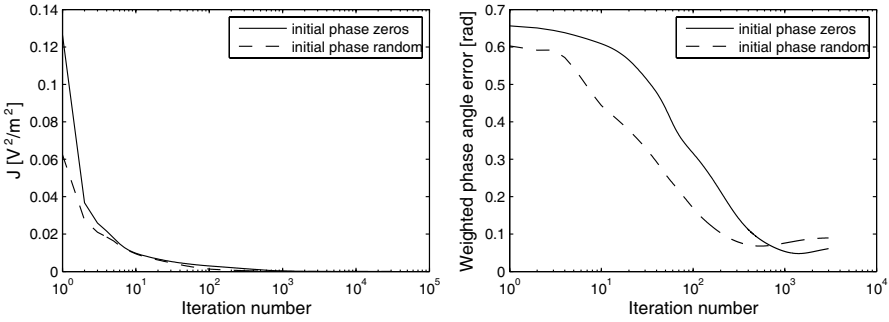

Figure 7. (a) The cost function J as function of iteration number for two cases with initial phase zeros and initial phase random numbers, respectively. (b) The summed and weighted phase angle errors as functions of iteration numbers for the two initial phase distributions.

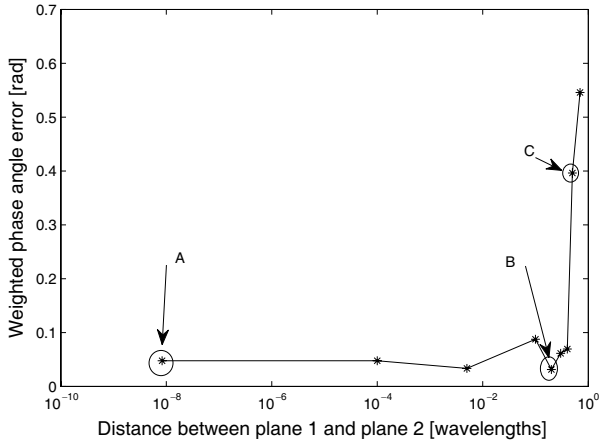

Figure 8. Summed and weighted phase angle error as function of the distance between plane 1 and plane 2.

Since the error becomes larger for the larger distances, one can wonder whether an increased resolution could improve the results. The resolution was therefore increased for the test case with the distance 0.5λ, but the resulting summed and weighted phase angle error did not become smaller.

It was also investigated how a change in the size of the measurement planes affects the result. The tests showed that if just the sides of the planes, for the test case with the distance 0.2λ between plane 1 and plane 2 (indicated as B in Figure 8), were increased by a factor 1.43, ϕ_{err} increased and became 0.97 rad instead of 0.031 rad. After the increase of the plane size the dimensions for the new test case, except the source, were scaled down with the same factor. That is the sides of the measurement planes, the distances between them and the distance to the source from the planes were all scaled down so that the distance between plane 1 and plane 2 became 0.1λ. Then ϕ_{err} became small again 0.097 rad. Thus it appears as though it may be harder to get good results, if the planes are too large in terms of wavelengths.

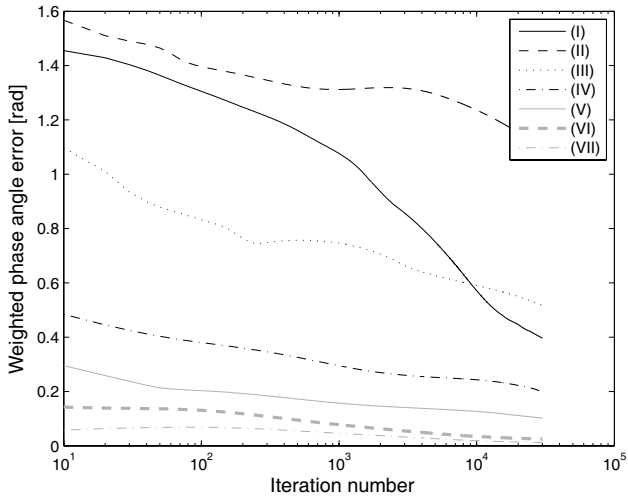

Figure 9. The obtained summed and weighted phase angle error as function of iteration number, for the test case with distance 0.5λ between plane 1 and plane 2. (I) Initial phase zeros, (II) initial phase random, (III) initial phase random, (IV) random interval -0.9π rad to 0.9π rad, (V) random interval -0.9π rad to 0.9π rad, (VI) random interval -0.8π rad to 0.8π rad, (VII) random interval -0.5π rad to 0.5π rad.

To investigate further what is happening for the test case with distance 0.5λ between the first two planes (indicated as C in Figure 8), the test case was run for some different initial phase distributions. The results can be found in Figure 9. One distribution with the initial value zero for all the phase angles (I) and two initial phase distributions with random phase, (II) and (III), were used. Four phase distributions with random numbers in different intervals (IV)–(VII) were also used. For the curves (IV)–(VII) it is written random interval and then an interval in the caption of the figure. These curves show results for different cases where the initial phase in each point is a random number in the specified interval around the correct phase from analytical formulas. The figure illustrates that small errors can be obtained for some of these intervals that are small enough, but for the other initial values the error becomes larger.

It can be noticed that the slope of the curve, for the case with initial phase angles zeros, is relatively steep near the last iteration. Therefore it is natural to consider whether the results can be improved if more iterations are run. Figure 10 shows how the summed and weighted phase angle error varies with the number of extra iterations, if the case with initial phase angles zeros is continued with more iterations. It was also tested if better results could be achieved if the phase was modified somewhat before the continuation of the simulation. The results for three different cases where the phase, before the extra iterations, in each point is set to a random number in an interval around the obtained phase for the first simulation part, are also shown in Figure 10. It can be seen that the errors for the four cases decrease with the number of extra iterations, but the resulting errors are still clearly larger than the results, for cases with smaller distances between plane 1 and plane 2, in Figure 8.

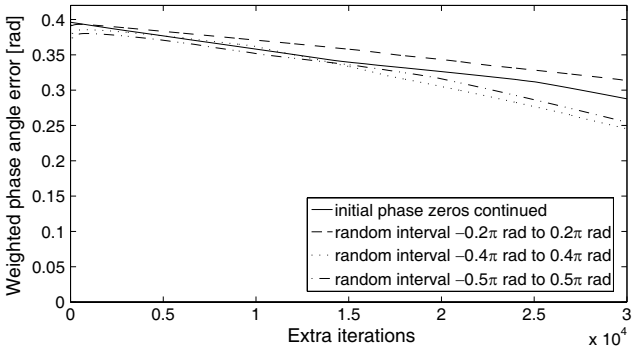

Figure 10. Summed and weighted phase angle error as function of the number of extra iterations.

4. DISCUSSION

The performance of the PAGM under different scenarios has been studied via numerical test cases. First, the test case with a source consisting of five infinitestimal dipoles was considered. The results showed that the PAGM is able to retrieve the phase information accurately with both initial zero and random phase distribution. Next, the performance of PAGM with a single dipole source at 50 Hz was tested via a number of different configurations. The sides of the plane and the separation distances between the planes were scaled and the summed and weighted phase angle error was evaluated. The results show that the error became larger if the dimensions became too large in terms of wavelengths.

On the other hand, however, the PAGM can accurately retrieve the phase information when the scaling factor is small, even if the separation between the planes are in the scale of $10^{-9}\lambda$. This is very useful if the measurements are performed very close to the source in terms of wavelengths. For low frequency applications the distance of a few wavelengths between the source and the measurement planes are hardly achievable in practice, then the PAGM provides an alternative solution for accurate phase retrieval.

We are also well aware that Isernia et al. [3] has looked into strategies to overcome the local minima problem for their method. It is reported that the distance between the scanning surfaces plays an important role in determining the lack or occurrence of local minima. Both the PAGM and the phase-retrieval method in [3] minimize a functional with a gradient based scheme. However, an important difference between the two methods is the choice of unknowns. In [3], the complex field that give the measured amplitudes on two planes is searched for and the functional is formulated so that the inverse problem becomes quadratic. In the PAGM, we instead search for the phase angles that together with measured field amplitudes on one measurement plane give correct calculated field amplitudes on two other planes. As a result, the PAGM does not have the same nonlinearity as the method in [3] and thus the results in [3] does not provide information about whether the PAGM works for cases with plane distances much smaller than the wavelength or not. Strictly speaking, phase retrieval of measurements with a few wavelengths separations and with measurements with sub-wavelength separations are two different problems with different solutions and thus they should be treated separately.

5. CONCLUSION

Performance of phase retrieval using the PAGM for different configurations has been evaluated. The results showed that the PAGM is able to accurately retrieve the phase information for test cases with different sources as well as various separations between and sizes of the measurement planes. More importantly, it is showed that the PAGM is able to accurately retrieve the phase information when the separations between the planes are much less than a wavelength. Such findings have not been widely reported in the open literature. The robustness of the PAGM is also tested for different initial phase distributions and it is found that the PAGM in general works for both zero phase setting and random settings. The findings from this work is very useful for phase reconstruction as well as complex source modeling for low-frequency applications such as electromagnetic dosimetry and complex source modeling.

ACKNOWLEDGMENT

The computations were performed on C3SE computing resources. The authors would also like to thank The Swedish Labour Market Insurance, AFA for their financial support to this project.

REFERENCES

1. Ayestarán, R. G., J. Laviada, and F. Las-Heras, "Realistic antenna array synthesis in complex environments using a MoM-SVR approach," *Journal of Electromagnetic Waves and Applications*, Vol. 23, No. 1, 97–108, 2009.
2. Isernia, T., G. Leone, and R. Pierri, "Results for a truncated phaseless near field technique," *Electronics Letters*, Vol. 29, No. 5, 505–506, Mar. 1993.
3. Isernia, T., G. Leone, and R. Pierri, "Radiation pattern evaluation from near-field intensities on planes," *IEEE Trans. Antennas and Propag.*, Vol. 44, No. 5, 701–710, May 1996.
4. Razavi, S. F. and Y. Rahmat-Samii, "A new look at phaseless planar near-field measurements: Limitations, simulations, measurements, and a hybrid solution," *IEEE Antennas and Propag. Magazine*, Vol. 49, No. 2, 170–178, Apr. 2007.
5. Yaccarino, R. G. and Y. Rahmat-Samii, "Phaseless bi-polar planar near-field measurements and diagnostics of array antennas," *IEEE Trans. Antennas and Propag.*, Vol. 47, No. 3, 574–583, Mar. 1999.

6. Las-Heras, F. and T. K. Sarkar, "A direct optimization approach for source reconstruction and NF-FF transformation using amplitude-only data," *IEEE Trans. Antennas and Propag.*, Vol. 50, No. 4, 500–510, Apr. 2002.
7. Hislop, G., G. C. James, and A. Hellicar, "Phase retrieval of scattered fields," *IEEE Trans. Antennas and Propag.*, Vol. 55, No. 8, 2332–2341, Aug. 2007.
8. Ribiere-Tharaud, N., M. Lambert, and P. Levesque, "Wideband validation of a phase retrieval process applied to infrared planar near-field measurements," *Progress In Electromagnetics Research B*, Vol. 23, 39–54, 2010.
9. Johansson, M., L. E. Nord, R. Kopecký, A. Fhager, and M. Persson, "Computational methods for modeling of complex sources," *COMPEL: The International Journal for Computation and Mathematics in Electrical and Electronic Engineering*, Vol. 27, No. 1, 133–143, 2008.
10. Johansson, M., H. S. Lui, and M. Persson, "Performance evaluation of phase retrieval method based on amplitude-only near-field data," *Proc. of Asia Pacific Microwave Conference*, 425–428, Singapore, Dec. 7–10, 2009.
11. Balanis, C. A., *Antenna Theory Analysis and Design*, John Wiley and Sons, Inc., New York, 1997.